Supporting Information

Defect tailoring in OH-functionalized carbon nanotubes for visible-light-driven ROS-mediated anticancer therapy and high-performance photocatalysis

Hyungbin Park,[‡,a,b] Sunyoung Hwang,[‡,c] Joowon Choi,[d] Kyungtae Kang,[,d] Hangil Lee,[*,c] and Seungwoo Hong,[*,a,b]*

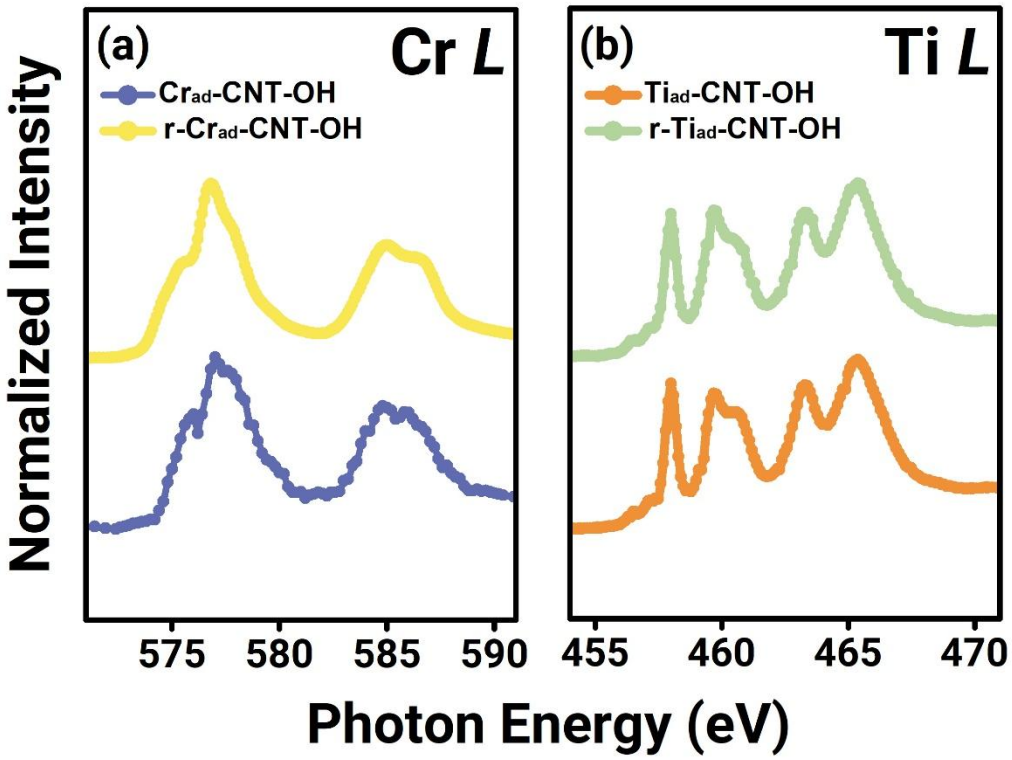

Fig. S1. XAS results of (a) Cr *L*-edges and (b) Ti *L*-edge XAS spectra of Cr_{ad}-CNT-OH (blue), r-Cr_{ad}-CNT-OH (yellow), Ti_{ad}-CNT-OH (orange), and r-Ti_{ad}-CNT-OH (green) samples.

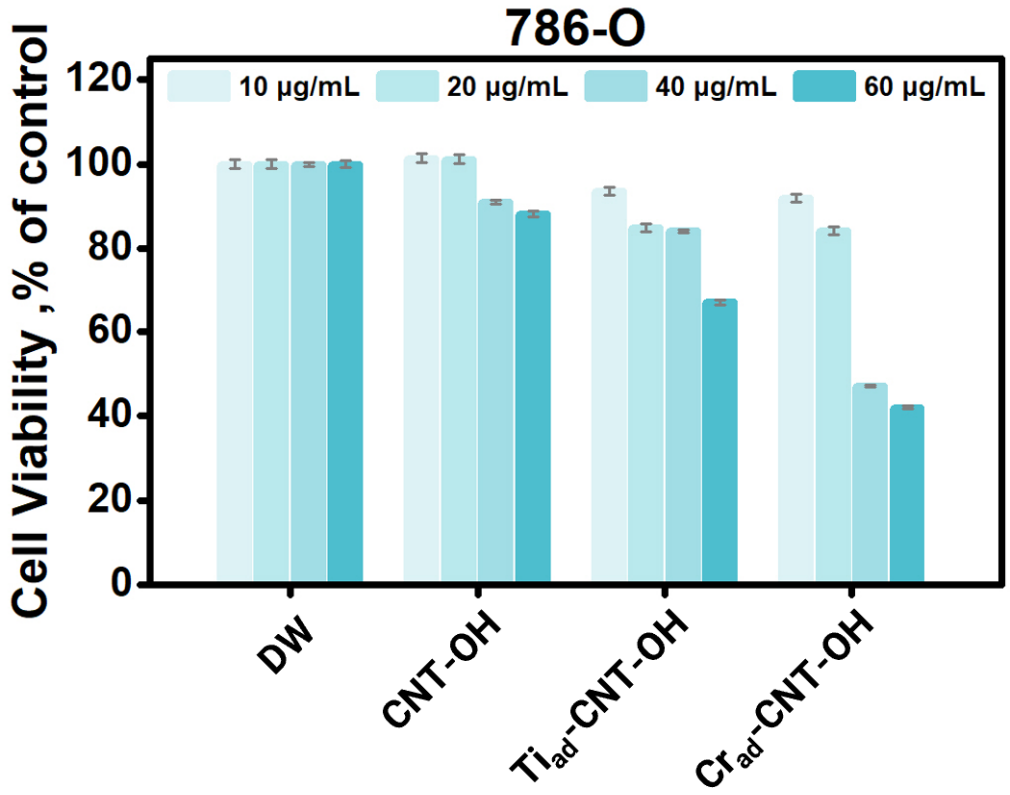

Fig. S2. 786-O cells were treated with different concentrations (10, 20, 40, and 60 µg/mL) of CNT–OH and TM_{ad}-CNT-OH (TM = Ti, and Cr), with 445 nm irradiation for 24 hours. Viability of cells without particle treatment and without irradiation was defined as 100%.

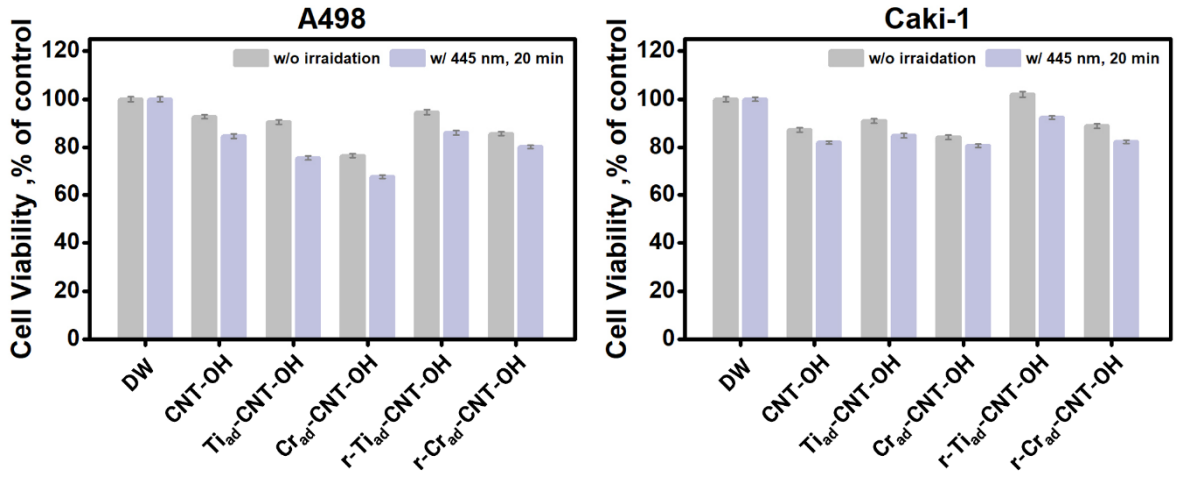

Fig. S3. Renal cancer cells (A498 and Caki-1) were treated with 40 μg/mL of CNT-OH, TM_{ad}-CNT-OH, and r-TM_{ad}-CNT-OH (TM = Ti, and Cr) with or without 445 nm irradiation, for 24 hours. The viability of cells without particles was defined as 100%.

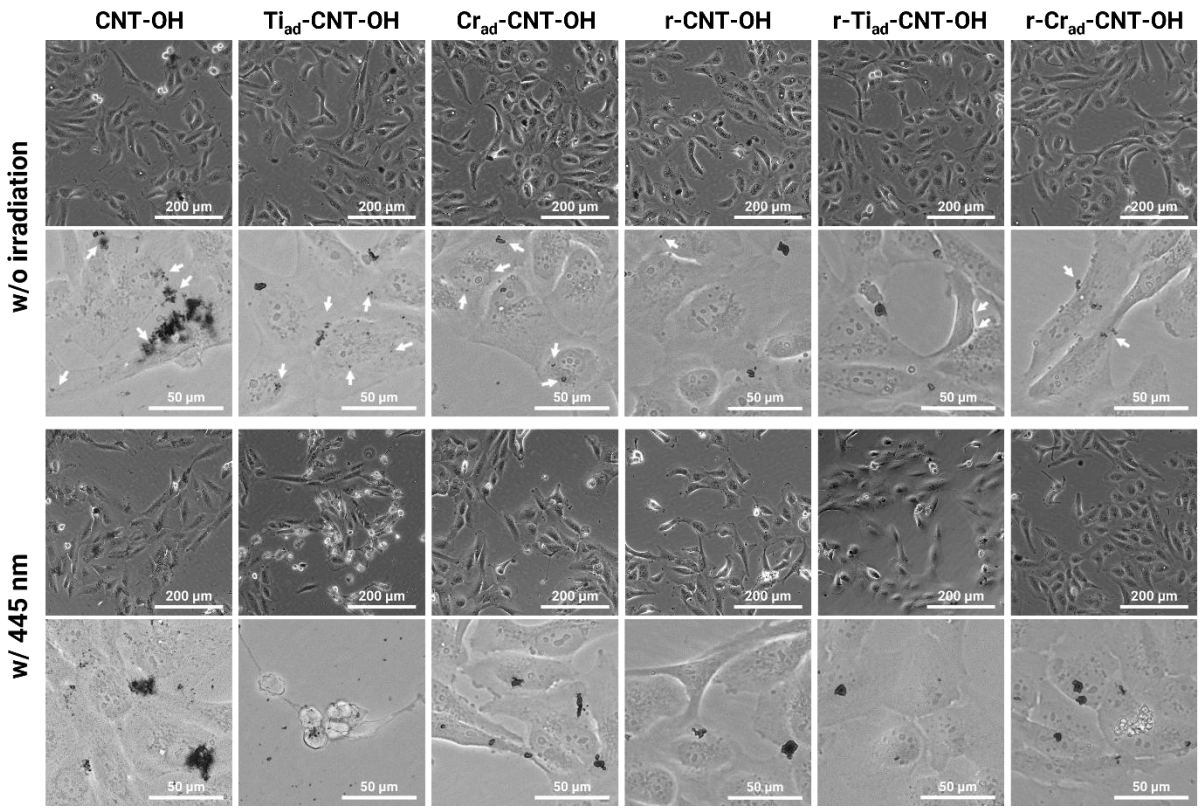

Fig. S4. Microscope images of 786-O cells treated with 20 μg/mL of CNT-OH, rCNT-OH, TM_{ad}-CNT-OH, and r-TM_{ad}-CNT-OH (TM = Ti, and Cr) with or without 445 nm irradiation for 24 hours. Scale bars: 200 μm and 50 μm.

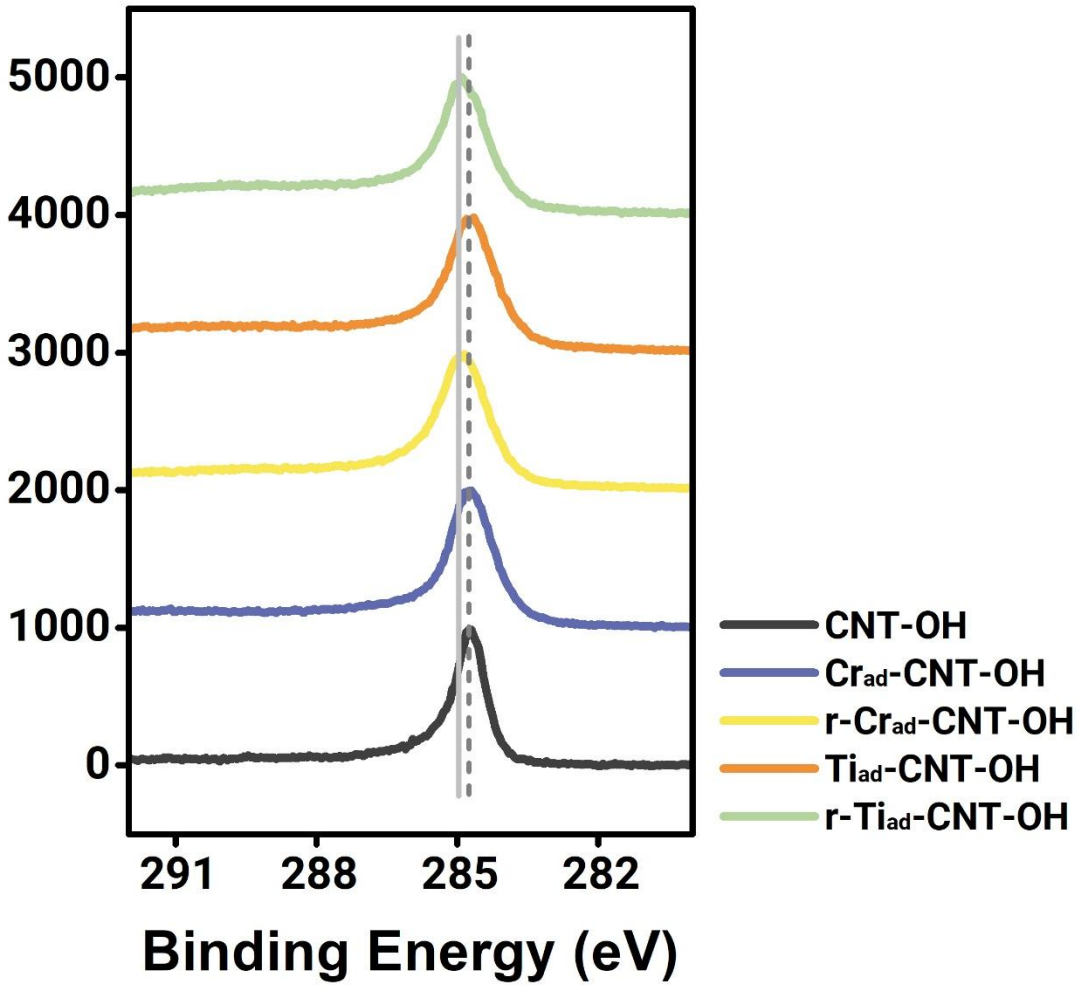

Fig. S5. C *K*-edges XAS spectra of the CNT-OH (black), Cr_{ad}-CNT-OH (blue), r-Cr_{ad}-CNT-OH (yellow), Ti_{ad}-CNT-OH (orange), and r-Ti_{ad}-CNT-OH (green) samples.

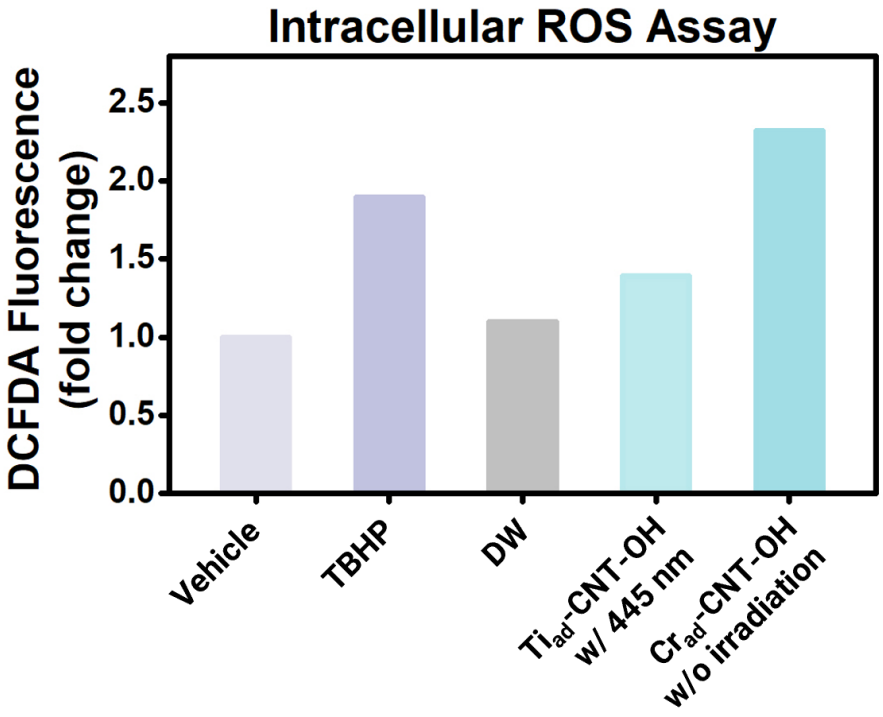

Fig. S6. DCFDA assays to measure intracellular ROS levels in 786-O cells treated with 40 μg/mL of Ti_{ad}-CNT-OH, Cr_{ad}-CNT-OH, and TBHP.

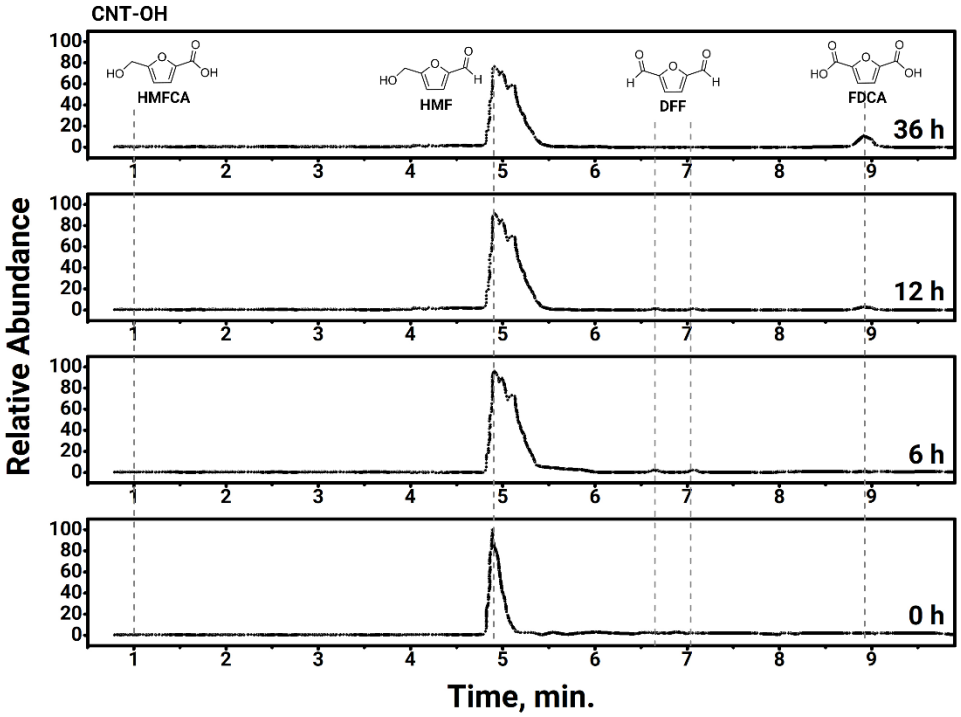

Fig. S7. HPLC-based product analysis for the selective oxidations of HMF by CNT-OH as functions of time when irradiated at 445 nm.

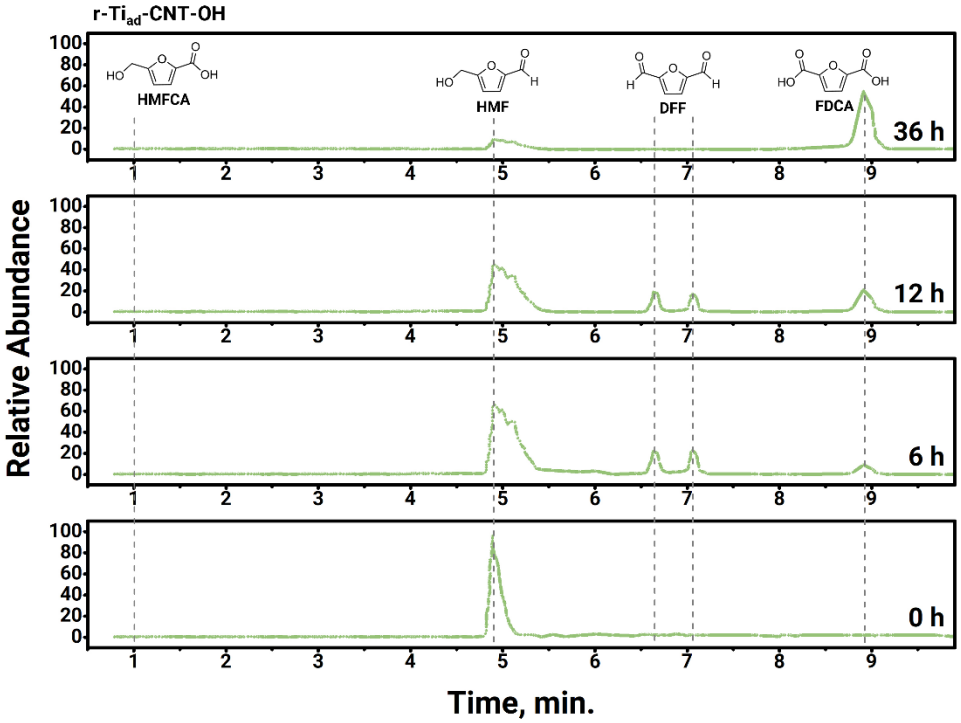

Fig. S8. HPLC-based product analysis for the selective oxidations of HMF by r-Ti_{ad}-CNT-OH as functions of time when irradiated at 445 nm.

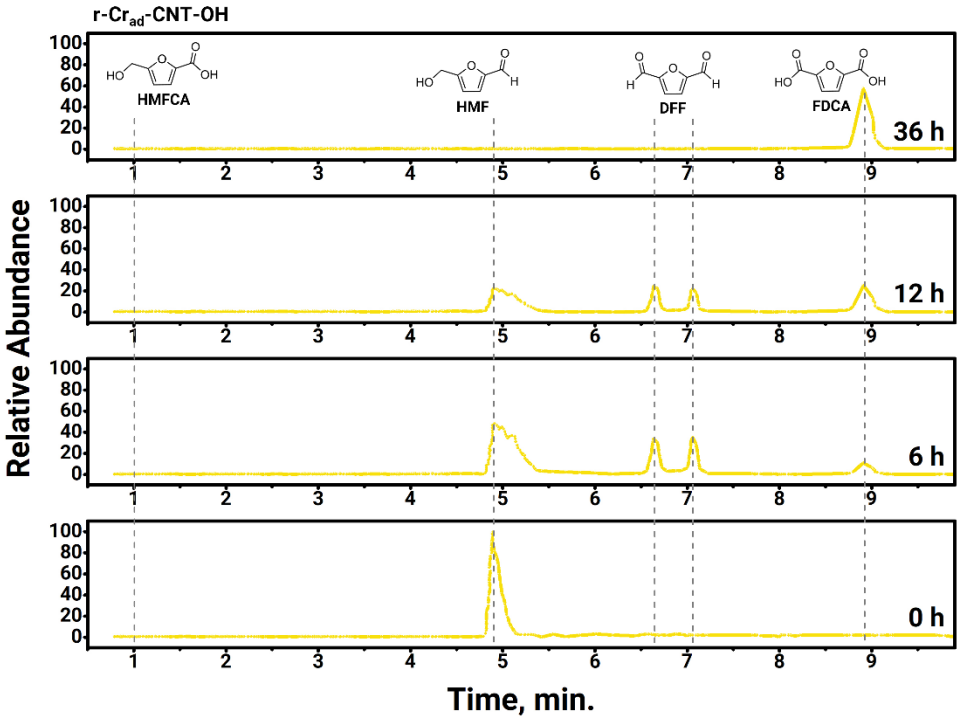

Fig. S9. HPLC-based product analysis for the selective oxidations of HMF by r-Cr_{ad}-CNT-OH as functions of time when irradiated at 445 nm.

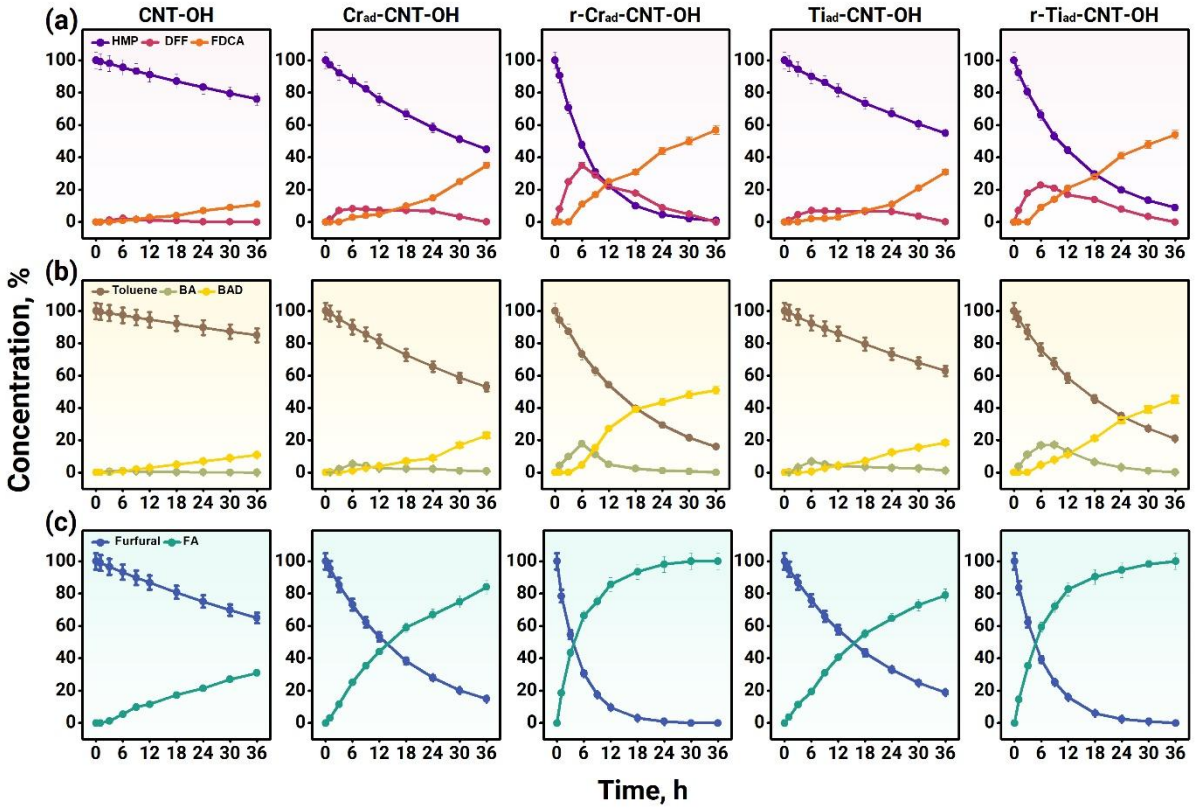

Fig. S10. HPLC-based product analysis for the selective oxidations of (a) HMF, (b) toluene, and (c) furfuraldehyde. Formation efficiencies for (a) FDCA from HMF via DFF, and (b) benzaldehyde from toluene via benzyl alcohol, and (c) Furoic acid from FA, as functions of time when irradiated at 445 nm. End-product yields over 36 h when irradiated at 445 nm.

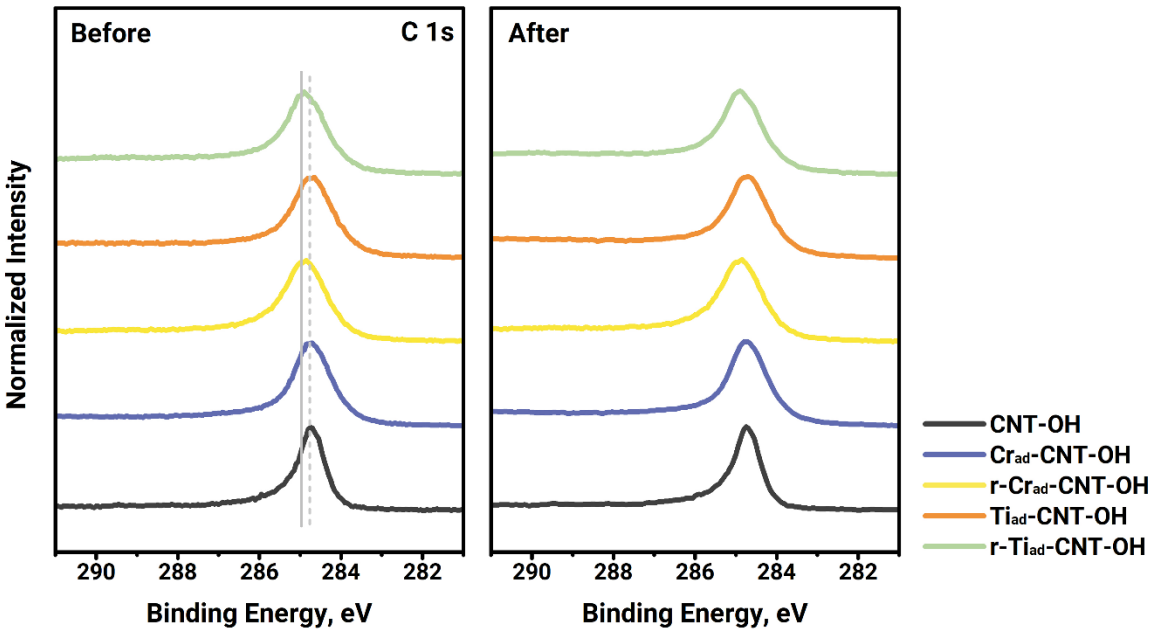

Fig. S11. C *K*-edges XAS spectra of the CNT-OH (black), Cr_{ad}-CNT-OH (blue), r-Cr_{ad}-CNT-OH (yellow), Ti_{ad}-CNT-OH (orange), and r-Ti_{ad}-CNT-OH (green) before (left panel) and after photocatalysis (right panel).

Table S1. Concentration yield of derivatives for photocatalytic conversion reaction for 36 h under visible light irradiation ($\lambda \geq 445$ nm) with 230 mW/cm^2 of illumination intensity

Samples	FDCA (%)	Benzaldehyde (%)	Furoic acid (%)
CNT-OH	11 ± 0.55	11 ± 0.55	31 ± 1.55
Cr_{ad}-CNT-OH	35 ± 1.75	23 ± 1.65	84 ± 4.2
r-Cr_{ad}-CNT-OH	57 ± 2.85	51 ± 2.55	100 ± 5.0
Ti_{ad}-CNT-OH	31 ± 1.55	19 ± 0.925	79 ± 3.95
r-Ti_{ad}-CNT-OH	54 ± 2.7	45 ± 2.27	100 ± 5.0

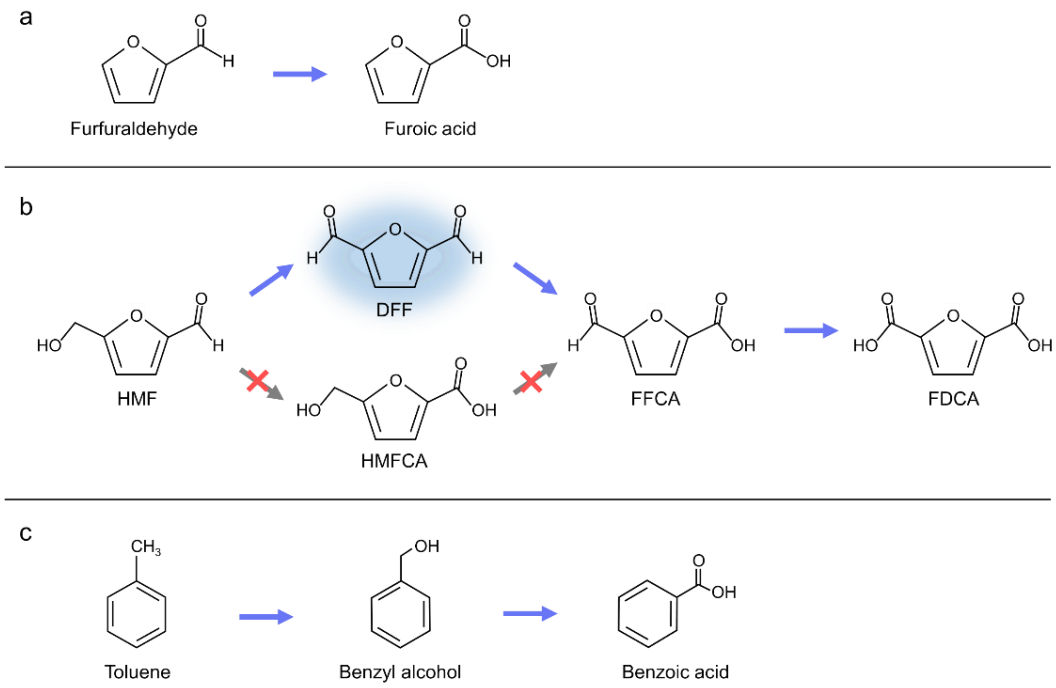

Scheme S1. Reaction pathway for the selective oxidation of (a) furfuraldehyde to furoic acid (FA), (b) HMF to FDCA via DFF, and (c) toluene to benzaldehyde via benzyl alcohol.